PHYSICAL REVIEW B VOLUME 27, NUMBER 7 1 APRIL 1983

# Reexamination of the third-order renormalization-group calculation for a one-dimensional interacting Fermi system

Chin-sen Ting, Xian-xi Dai, and Bambi Hu
*Department of Physics, University of Houston, Houston, Texas 77004*
(Received 14 June 1982)

A one-dimensional interacting Fermi system with weak-coupling parameters $g_1$ ($<0$) and $g_2$ is reexamined in the third-order renormalization-group approach. Our result indicates that the value of the invariant coupling $g_1'$ varies, depending on whether the limit $\omega\to 0$, $q=0$ or $\omega=0$, $q\to 0$ is taken. For $\omega\to 0$, $q=0$, the invariant coupling $g_1'$ scales to $g_1'/\pi v\simeq -1.24$, and for $\omega=0$, $q\to 0$, it scales to $g_1'/\pi v\simeq -0.716$. We also argue that the invariant coupling $g_1'$ obtained from neither limit is appropriate for calculating the critical exponents of various response functions.

## I. INTRODUCTION

During the past several years there have been extensive theoretical studies of the properties of a one-dimensional interacting Fermi system.[1-15] Among these different approaches, the method of perturbative renormalization group has been applied to the system, and it seems quite successful in predicting the ground state for such a system with restricted values of interacting parameters.[5,10] The preliminary work of applying the perturbative renormalization-group approach was carried out by Menyhard and Sólyom[4,5] up to second-order or two-loop calculations. One essential feature of their results is that with the backscattering interaction $g_1<0$ and the Tomonaga-type interaction $g_2$ small, the invariant coupling $g_1'$ is scaled to the value $g_1'/\pi v=-2$ in the low-frequency limit, where $v$ is the particle velocity at the Fermi level. Another feature of their calculation is that the value of $g_1'-2g_2'$ is a scale invariant.

Since the invariant coupling $g_1'/\pi v=-2$ obtained for $g_1<0$ in the second-order renormalization-group calculation is quite large, using it to calculate those response functions[5] which can only be obtained in powers of $g_1'$ and $g_2'$ seems to be unjustified. Carrying $g_1'$ to a higher order was therefore necessary. The application of the third-order renormalization-group method to evaluate $g_1'$ and $g_2'$ was first studied by Ting.[12] In the previous work[12] the scale invariance of $g_1'-2g_2'$ is destroyed by the presence of a small term $\alpha$ in Eqs. (52) and (53) of Ref. 12. In evaluating those fourth-order diagrams[12] for the vertex functions, the values for most of the graphs depend not only on how the momentum-transfer cutoffs in the multiple momentum integrations are chosen but also on how the external frequencies are arranged on the vertex functions. These artificial effects in our calculation almost cancel when the contributions from each of the graphs are summed up. We believe that the presence of the parameter $\alpha$ might be either due to not enough accuracies in the calculation or improper choice of momentum cutoffs which might violate the particle-hole symmetry of the Hamiltonian.[13] If the small term $\alpha$ ($=4\ln 2-3\ln 3$) is neglected there, then $g_1'-2g_2'$ indeed becomes scale invariant. The result[12] shows that $g_1'$ has a fixed point and in the weak-coupling limit it scales to $g_1'/\pi v\simeq -0.87$, when $g_1'$ is used for calculating the critical exponents of various fluctuation response functions. Recently Rezayi, Sak, and Talukdar[16] have repeated our calculation by using a similar approach and they are able to show explicitly that $g_1'-2g_2'$ is a scale invariant. However, their result for $g_1'$ in the low-frequency limit, contrary to that of Ref. 12, does not have a real fixed point for $g_1'<0$. This difference as pointed out by the authors in Ref. 16 is primarily due to the choice of momentum cutoffs in the multiple momentum integrations. In the work of Ref. 12 the bandwidth momentum-cutoff procedure was used, while in Ref. 16 the transfer momentum-cutoff procedure was adopted. In this paper the problem shall be reexamined by using the bandwidth momentum cutoffs. We shall show that in the weak-coupling limit for $g_1'<0$ the invariant coupling $g_1$ scales to $g_1'/\pi v\simeq -1.24$ as $\omega\to 0$, $q=0$ and to $g_1'/\pi v\simeq -0.716$ as $\omega=0$, $q\to 0$. Namely the value of $g_1'$ in the limit of low frequency is different from that of $g_1'$ in the limit of long wavelength. We shall also argue that the value of $g_1'$ used for calculating the low-frequency response functions should be $g_1'/\pi v\simeq -0.87$, which is the result that we obtained previously in Ref. 12.

 ©1983 The American Physical Society

## II. DESCRIPTION OF THE MODEL AND THE RENORMALIZATION-GROUP EQUATION

The model used here for discussion is identical to that described in Refs. 4 and 12. We used the following Hamiltonian for the one-dimensional interacting Fermi system:

$$H=\sum_{k,\alpha}\epsilon_k(a^\dagger_{k\alpha}a_{k\alpha}+b^\dagger_{k\alpha}b_{k\alpha})+H_{\rm int}\ , \tag{1}$$

$$H_{\rm int}=\frac{g_1}{L}\sum a^\dagger_{k_1\alpha}b^\dagger_{k_2\beta}a_{k_3\beta}b_{k_1+k_2-k_3,\alpha}+\frac{g_2}{L}\sum a^\dagger_{k_1\alpha}b^\dagger_{k_2\beta}b_{k_3\beta}a_{k_1+k_2-k_3,\alpha}\ , \tag{2}$$

where $a^\dagger_{k_i\alpha}$ and $b^\dagger_{k_i\alpha}$ create particles with spin $\alpha$, momenta $k_F-k_c<k_i<k_F+k_c$, and $-k_F-k_c<k_i<-k_F+k_c$, respectively. The cutoff momentum $k_c$ is related to $\omega_D$ by $vk_c=\frac{1}{2}\omega_D$; here $v$ is the Fermi velocity. $\epsilon_k=v(|k|-k_F)$ is the kinetic energy of the particle. $g_1$ represent the interaction with momentum transfer near $2k_F$, and $g_2$ with momentum transfer near 0. The renormalized interaction or the vertex function $\Gamma_{\alpha\beta,\gamma\delta}(k_1\omega_1,k_2\omega_2,k_3\omega_3,k_4\omega_4)$ depends on three independent momenta and three independent frequencies, which have been chosen in such a way[4] that

$$\begin{aligned}&k_1=k_4=-k_F,\ \ k_2=k_3=k_F\ ,\\&\omega_1=\tfrac{3}{2}\omega,\ \ \omega_2=-\tfrac{1}{2}\omega,\ \ \omega_3=\omega_4=\tfrac{1}{2}\omega\ .\end{aligned} \tag{3}$$

As pointed out by authors in Ref. 4 that exactly the same results for the logarithmic divergent terms would be obtained if all the frequencies are chosen to be zero and keeping a single momentum variable $q$, for example,

$$\begin{aligned}&\omega_1=\omega_2=\omega_3=\omega_4=0\ ,\\&k_1=-k_F,\ \ k_2=k_F+q\ ,\\&k_3=k_F-q,\ \ k_4=-k_F+2q\ .\end{aligned} \tag{4}$$

We shall show at the latter part of this paper that this different choice of energy and momentum variables may lead to different results for the third-order renormalization-group equation. For the moment, let us make the choice according to Eq. (3). The vertex function $\Gamma$ yields in general a spin structure

$$\Gamma_{\alpha\gamma,\beta\delta}(\omega)=g_1\tilde{\Gamma}_1(\omega)\delta_{\alpha\gamma}\delta_{\beta\delta}-g_2\tilde{\Gamma}_2(\omega)\delta_{\alpha\delta}\delta_{\beta\gamma}\ . \tag{5}$$

The renormalized Green function $G$ is related to the bare Green function $g(\pm k_F,\omega)$:

$$G(\pm k_F,\omega)=d(\omega/\omega_D,g_1,g_2)g(\pm k_F,\omega)\ . \tag{6}$$

The detailed description of the renormalization-group method has been given previously.[4,12] Here we need only to write down the scaling relations and renormalization-group equations according to Ref. 4. By changing the energy cutoff from $\omega_D$ to $\omega_D'$ and simultaneously the couplings $g_1,g_2$ to $g_1',g_2'$, multiplicative renormalization means that the Green function and the vertex functions transform as

$$d(\omega/\omega_D',g_1',g_2')=z_1d(\omega/\omega_D,g_1,g_2)\ , \tag{7}$$

$$\tilde{\Gamma}_1(\omega/\omega_D',g_1',g_2')=z_2^{-1}\tilde{\Gamma}_1(\omega/\omega_D,g_1,g_2)\ , \tag{8}$$

$$\tilde{\Gamma}_2(\omega/\omega_D',g_1',g_2')=z_3^{-1}\tilde{\Gamma}_2(\omega/\omega_D,g_1,g_2)\ , \tag{9}$$

$$g_1'=z_1^{-2}z_2g_1,\ \ g_2'=z_1^{-2}z_3g_2\ , \tag{10}$$

where the $z_i$'s are real and independent of $\omega$. Therefore, the $z_i$'s can be obtained from the above equations by setting $\omega=\omega_D'$.

The prescription of the renormalization-group method is that, for any quantity $\tilde{A}$ obeying the multiplicative renormalization condition

$$\tilde{A}(\omega/\omega_D',g_1',g_2')=z\tilde{A}(\omega/\omega_D,g_1,g_2)\ , \tag{11}$$

the Lie equation of the group can be derived as[17]

$$\frac{\partial}{\partial x}\ln\tilde{A}(x,g_1,g_2)=\frac{1}{x}\left[\frac{\partial}{\partial\xi}\ln\tilde{A}(\xi,g_1',g_2')\right]_{\xi=1}\ , \tag{12}$$

where $x=\omega/\omega_D$. The labor involved in the renormalization-group calculation is the evaluation of the right-hand side of the above equation by perturbation theory for $\omega=\omega_D$ ($\xi=1$).

## III. RENORMALIZING CONSTANTS AND INVARIANT COUPLINGS

The third-order self-energy and the fourth-order (or three-loop) diagrams for the vertex functions have been calculated previously.[12] The constants $z_i$ in the third-order renormalization have been shown to have the following expressions[12]:

$$z_1^{-1}=1+\frac{1}{(2\pi v)^2}(g_1^2-g_1g_2+g_2^2)\ln\left[\frac{\omega_D'}{\omega_D}\right]+\frac{3}{2(2\pi v)^3}g_1^3\ln^2\left[\frac{\omega_D'}{\omega_D}\right]-\frac{3}{2(2\pi v)^3}g_1^3\ln\left[\frac{\omega_D'}{\omega_D}\right]\ , \tag{13}$$

$$z_2 = 1+\frac{1}{\pi v}g_1\ln\left[\frac{\omega_D'}{\omega_D}\right]+\frac{1}{(\pi v)^2}g_1^2\ln^2\left[\frac{\omega_D'}{\omega_D}\right]+\frac{1}{(\pi v)^3}g_1^3\ln^3\left[\frac{\omega_D'}{\omega_D}\right]+\frac{1}{2(\pi v)^2}(g_1g_2-g_2^2)\ln\left[\frac{\omega_D'}{\omega_D}\right]$$
$$+\frac{1}{8(\pi v)^3}(3g_1^3+4g_1^2g_2-4g_1g_2^2)\ln^2\left[\frac{\omega_D'}{\omega_D}\right]+a_2\ln\left[\frac{\omega_D'}{\omega_D}\right], \tag{14}$$

$$z_3 = 1+\frac{1}{g_2}\left[\frac{1}{2(\pi v)}g_1^2\ln\left[\frac{\omega_D'}{\omega_D}\right]+\frac{1}{2(\pi v)^2}g_1^3\ln^2\left[\frac{\omega_D'}{\omega_D}\right]+\frac{1}{2(\pi v)^3}g_1^4\ln^3\left[\frac{\omega_D'}{\omega_D}\right]\right.$$
$$+\frac{1}{4(\pi v)^2}(g_1^3-2g_1^2g_2+2g_1g_2^2-2g_2^3)\ln\left[\frac{\omega_D'}{\omega_D}\right]+\frac{1}{8(\pi v)^3}(3g_1^4-g_1^3g_2-2g_1^2g_2^2)\ln^2\left[\frac{\omega_D'}{\omega_D}\right]$$
$$\left.+a_3g_2\ln\left[\frac{\omega_D'}{\omega_D}\right]\right]. \tag{15}$$

However, the results for the coefficients $a_2$ and $a_3$ obtained by Ting[12] and by the more recent calculation[16] seem not to agree with each other. Before we point out the origin of this difference, let us briefly discuss which diagrams are contributing to $a_2$ and $a_3$. If those terms due to the artificial effects by making the choice of momentum-transfer cutoffs in the multiple momentum integrations and the arrangement of the external frequencies on the vertex functions are neglected,[18] it is straightforward to show that diagrams which contribute to $a_i$ and $a_i$ are given by Fig. 4(i) of Ref. 12 and all the graphs listed in Figs. 6 and 7 of Ref. 12. The method used to evaluate all the graphs in Ref. 12 is to restrict the momentum associated with each Green function in the region $(k_c,-k_c)$. We call this type of restriction on momentum integration as the bandwidth cutoff. In Ref. 16, however, the authors there used the transfer cutoff method which restricts the momentum transfer between two electrons or the momentum associated with each interaction line in the region $(k_c,-k_c)$. A careful examination indicates that the results obtained in Ref. 16 for most of the graphs mentioned above are identical to Ting,[12] except for the graphs listed in Fig. 1. The values of graphs from 1(a) to 1(e) are separately equal to zero if the choice of the momentum and energy variables on the vertex functions is made according to Eq. (3). The identical conclusion has also been reached by the authors in Ref. 16. In the previous work,[12] however, finite values have been assigned to these graphs; the reason will be given later. For the moment let us take the values of graphs from 1(a) to 1(e) separately equal to zero. The only disagreement left are the values for those graphs from (f) to (i) of Fig. 1. It is straightforward to show that the value of graphs 1(f) and 1(g) is identical to that of graph 1(h) and 1(i); the sum of their contributions to the vertex functions has already been given[12]:

$$\gamma^{(1fghi)} = 2(g_1^2-g_1g_2+g_2^2)(2g_1^2\delta_{\alpha\gamma}\delta_{\beta\delta}-g_1^2\delta_{\alpha\delta}\delta_{\beta\gamma})\frac{1}{2}\frac{1}{(2\pi v)^3}\left[\ln^2\left[\frac{\omega}{\omega_D}\right]-(1+i\pi)\ln\left[\frac{\omega}{\omega_D}\right]\right]. \tag{16}$$

The recent calculation by the authors of Ref. 16 shows a slightly different result for these sets of graphs; they obtain

$$\gamma^{(1fghi)} = 2(g_1^2-g_1g_2+g_2^2)(2g_1^2\delta_{\alpha\gamma}\delta_{\beta\delta}-g_1^2\delta_{\alpha\gamma}\delta_{\beta\gamma})\frac{1}{2}\frac{1}{(2\pi v)^3}\left[\ln^2\left[\frac{\omega}{\omega_D}\right]-(-1+i\pi)\ln\left[\frac{\omega}{\omega_D}\right]\right]. \tag{17}$$

Namely, the real part of the coefficient in front of $\ln(\omega/\omega_D)$ has an opposite sign as compared with Ref. 12. The calculation has been checked again and we concluded[16] that this discrepancy exists because in Ref. 12 the bandwidth cutoff method was used while in Ref. 16 the authors used the transfer cutoffs. Because of this difference, the result of Ref. 16 for $g_1'$ does not have a real fixed point for $g_1<0$, or the value of $g_1'$ becomes divergent in the low-frequency limit. In the following we shall apply

the bandwidth cutoffs[12] for the momentum integrations in evaluating those Feynman diagrams. It would be useful to write down the vertex functions $\tilde{\Gamma}_1(\omega)$ and $\tilde{\Gamma}_2(\omega)$ as defined in Eq. (5) up to third-order terms in $g_1'$ or $g_2$. In order to make our later discussion more convenient and transparent, we shall discard the imaginary parts associated with those diagrams which represent the vertex functions, and terms due to the momentum-cutoff procedures. This simplication may not be necessary, but it is equivalent to the simpler one of the two methods proposed in Ref. 16. In the Appendix the results for the vertex diagrams which have been evaluated in Ref. 12 will be listed again in their simplified forms. From the Appendix the vertex functions $\tilde{\Gamma}_1(\omega)$ and $\tilde{\Gamma}_2(\omega)$ have the following expressions[19]:

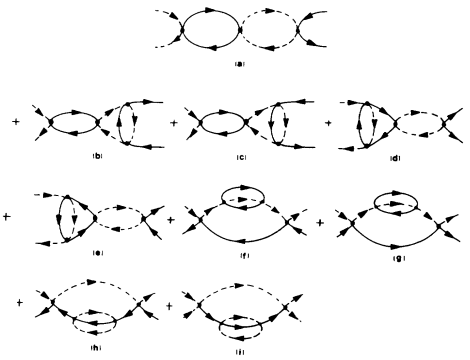

FIG. 1. Some graphs representing the vertex parts. The black dots are the bare interactions defined in Eq. (2). The dashed lines and the solid lines are, respectively, the Green function with momentum near $-k_F$ and $+k_F$.

$$\tilde{\Gamma}_1(\omega)=1+\frac{g_1}{\pi v}\ln\left[\frac{\omega}{\omega_D}\right]+\frac{g_1^2}{(\pi v)^2}\ln^2\left[\frac{\omega}{\omega_D}\right]+\frac{g_1^3}{(\pi v)^3}\ln^3\left[\frac{\omega}{\omega_D}\right]+\frac{1}{2(\pi v)^2}(g_1g_2-g_2^2)\ln\left[\frac{\omega}{\omega_D}\right]$$
$$+\frac{1}{8(\pi v)^3}(3g_1^3+4g_1^2g_2-4g_1g_2^2)\ln^2\left[\frac{\omega}{\omega_D}\right]+b_1\ln\left[\frac{\omega}{\omega_D}\right]+c_1\ , \tag{18}$$

$$\tilde{\Gamma}_2(\omega)=1+\frac{g_1^2}{2(\pi v)g_2}\ln\left[\frac{\omega}{\omega_D}\right]+\frac{g_1^3}{2(\pi v)^2g_2}\ln^2\left[\frac{\omega}{\omega_D}\right]+\frac{g_1^4}{2(\pi v)^3g_2}\ln^3\left[\frac{\omega}{\omega_D}\right]$$
$$+\frac{1}{4(\pi v)^2g_2}(g_1^3-2g_1^2g_2+2g_1g_2^2-2g_2^3)\ln\left[\frac{\omega}{\omega_D}\right]+\frac{1}{8(\pi v)^3g_2}(3g_1^4-g_1^3g_2-2g_1^2g_2^2)\ln^2\left[\frac{\omega}{\omega_D}\right]$$
$$+b_2\ln\left[\frac{\omega}{\omega_D}\right]+c_2\ , \tag{19}$$

where the constants $c_1$ and $c_2$ are contributions entirely from graph (a) of Fig. 1; in the present limit $\omega\to 0$ and $q=0$, $c_1=c_2=0$. The constants $b_1$ and $b_2$ are proportional to the third power of $g_1$ and $g_2$ and they can, respectively, be written as

$$b_1=\frac{1}{(2\pi v)^3}[2g_1(g_1g_2-g_2^2)+2g_1^3+\beta_1]\ , \tag{20}$$

$$b_2=\frac{1}{(2\pi v)^3}\left[4g_1^3-\frac{g_1^2}{g_2}(\tfrac{1}{2}g_1^2+g_2^2)+\beta_2\right]\ . \tag{21}$$

The constants $\beta_1$ and $\beta_2$ here are entirely from graphs (f) to (i) of Fig. 1. Neglecting the imaginary part on the right-hand side of Eq. (16), the following results are obtained for $\beta_1$ and $\beta_2$:

$$\beta_1=-2g_1(g_1^2-g_1g_2+g_2^2)\ , \tag{22}$$

$$\beta_2=-\frac{g_1^2}{g_2}(g_1^2-g_1g_2+g_2^2)\ . \tag{23}$$

Substituting them into Eqs. (20) and (21), we have

$$b_1=\frac{1}{(2\pi v)^3}[4g_1(g_1g_2-g_2^2)]\ , \tag{24}$$

$$b_2=\frac{1}{(2\pi v)^3}\left[5g_1^3-\frac{g_1^2}{g_2}(\tfrac{3}{2}g_1^2+2g_2^2)\right]\ . \tag{25}$$

By setting $\omega_D=\omega_D'$ in Eqs. (8) and (9), the renormalizing constants $z_2$ and $z_3$ can be shown to be given by Eqs. (14) and (15) with $a_2=b_1$ and $a_3=b_2$. The invariant couplings $g_1'$ and $g_2'$ are then determined from Eq. (10) together with the expression for $z_1$ [see Eq. (13)]. It is straightforward to show that

$$g_1'=\bar{g}_1+\frac{1}{(2\pi v)^3}[-3g_1^4+4g_1^2(g_1g_2-g_2^2)]$$
$$\times\ln\left[\frac{\omega_D'}{\omega_D}\right]\ , \tag{26}$$

$$g_2' = \bar{g}_2 + \frac{1}{2(2\pi v)^3}[-3g_1^4 + 4g_1^2(g_1 g_2 - g_2^2)] \times \ln\left[\frac{\omega_D'}{\omega_D}\right], \tag{27}$$

with $\bar{g}_1$ and $\bar{g}_2$ given, respectively, by

$$\bar{g}_1 = g_1 + \frac{g_1^2}{\pi v}\ln\left[\frac{\omega_D'}{\omega_D}\right] + \frac{g_1^3}{(\pi v)^2}\ln^2\left[\frac{\omega_D'}{\omega_D}\right] + \frac{g_1^4}{(\pi v)^3}\ln^3\left[\frac{\omega_D'}{\omega_D}\right] + \frac{g_1^3}{2(\pi v)^2}\ln\left[\frac{\omega_D'}{\omega_D}\right] + \frac{5g_1^4}{4(\pi v)^3}\ln^2\left[\frac{\omega_D'}{\omega_D}\right], \tag{28}$$

$$\bar{g}_2 = g_2 + \frac{g_1^2}{2(\pi v)}\ln\left[\frac{\omega_D'}{\omega_D}\right] + \frac{g_1^3}{2(\pi v)^2}\ln^2\left[\frac{\omega_D'}{\omega_D}\right] + \frac{g_1^4}{2(\pi v)^3}\ln^3\left[\frac{\omega_D'}{\omega_D}\right] + \frac{g_1^3}{4(\pi v)^2}\ln\left[\frac{\omega_D'}{\omega_D}\right] + \frac{5g_1^4}{8(\pi v)^3}\ln^2\left[\frac{\omega_D'}{\omega_D}\right]. \tag{29}$$

Here we wish to point out that the results of Rezayi *et al.*[16] for $g_1'$ and $g_2'$ can be exactly obtained if one uses Eq. (17) or simply changes the sign of $\beta_1$ and $\beta_2$ defined in Eqs. (22) and (23). It is noted that $g_2' - \frac{1}{2}g_1' = g_2 - \frac{1}{2}g_1$ is invariant under the renormalization-group transformation. Within the validity of the third-order renormalization, the invariant coupling $g_1'$ satisfies the following equation:

$$\frac{\partial}{\partial x}\ln g_1'(x) = \frac{1}{x}\left[\frac{1}{\pi v}\left[1 - \frac{\delta^2}{2}\right]g_1'(x) + \frac{g_1'^2(x)}{2(\pi v)^2} - \frac{1}{4(\pi v)^3}g_1'^3(x)\right], \tag{30}$$

here $x = \omega/\omega_D$ and $\delta = (g_2 - g_1/2)/\pi v$. In order to obtain the above equation, the relation $g_2' = g_2 - \frac{1}{2}g_1 + \frac{1}{2}g_1'$ has been used. We shall work in the limit $\delta \ll 1$, that is, either in the weak-coupling limit ($g_1, g_2 \ll \pi v$) or in the region where $g_1' \sim 2g_2$ as $\omega \to 0$; it is easy to show that $g_1'/\pi v$ scales to a fixed value $g_1'/\pi v = -(\sqrt{5}-1)$ ($\simeq -1.24$).

In our discussion above, the momenta and frequencies that appeared in the vertex functions have been chosen according to Eq. (3), that is, in the limit $\omega \to 0$, $q = 0$. The only variable is the frequency $\omega$. If the other choice which is given by Eq. (4) is made or in the limit $\omega = 0$, $q \to 0$, the only variable is the single momentum $q$. It is easy to show that exactly the same results for the logarithmic divergent terms would be obtained simply by replacing $\omega$ with $vq$.[4] However, each value of those diagrams from 1(a) to 1(e) which was zero previously is now finite. This is because each of these graphs consists of at least one Landau bubble; for small $\omega$ and $q$ each Landau bubble contributes a term $L_B$:

$$L_B = \frac{1}{2\pi v}\frac{vq}{\omega - vq} = \begin{cases} 0, & \omega \to 0,\ q = 0 \\ -1/2\pi v, & \omega = 0,\ q \to 0 \end{cases}. \tag{31}$$

Its value, unlike those logarithmic divergent terms, depends critically on how $\omega$ and $q$ are approaching zero. For $\omega = 0$ and $q \to 0$ the correction to the vertex functions from graphs 1(a) can easily be obtained,

$$\gamma^{(1a)} = [g_1^3\delta_{\alpha\gamma}\delta_{\beta\delta} - (3g_1^2 g_2 - 6g_1 g_2^2 + 4g_2^3)\delta_{\alpha\delta}\delta_{\beta\gamma}]\frac{1}{(2\pi v)^2}. \tag{32}$$

Summing the contributions from graph 1(b)–1(e), we have

$$\gamma^{(1bcde)} = -(2g_1^4\delta_{\alpha\gamma}\delta_{\beta\delta} - g_1^4\delta_{\alpha\delta}\delta_{\beta\gamma}) \times \frac{1}{(2\pi v)^3}\ln\left[\frac{vq}{\omega_D}\right]. \tag{33}$$

Thus in the limit of $q \to 0$ and $\omega = 0$, there are extra terms from Eqs. (32) and (33) which should be added to our previous vertex functions. By replacing $\omega$ with $vq$ in Eqs. (18) and (19), and adding the contributions from Eqs. (32) and (33) to $\tilde{\Gamma}_1(vq)$ and $\tilde{\Gamma}_2(vq)$, we have

$$b_1 = \frac{1}{(2\pi v)^3}[-2g_1^3 + 4g_1(g_1 g_2 - g_2^2)], \tag{34}$$

$$b_2 = \frac{1}{(2\pi v)^3}\left[5g_1^3 - \frac{g_1^2}{g_2}(\tfrac{5}{2}g_1^2 + 2g_2^2)\right]. \tag{35}$$

The constants $c_1$ and $c_2$, which were previously zero, now become

$$c_1 = \frac{1}{(2\pi v)^2}g_1^2, \tag{36}$$

$$c_2 = \frac{1}{(2\pi v)^2}(3g_1^2 - 6g_1 g_2 + 4g_2^2). \tag{37}$$

With the use of the multiplicative renormalization Eqs. (8) and (9), the constants appearing in $z_2$ and $z_3$ can be obtained as

$$a_2 = \frac{1}{(2\pi v)^3}[-8g_1^3 + 4(g_1^2 g_2 - g_1 g_2^2)], \tag{38}$$

$$a_3 = \frac{1}{(2\pi v)^3}\frac{1}{2g_2}(-11g_1^4 + 10g_1^3 g_2 - 4g_1^2 g_2^2). \tag{39}$$

From Eq. (10) the invariant couplings $g_1'$ and $g_2'$ in the limit of $\omega=0$ and finite but small $q$ can be shown to have the forms

$$g_1'=\bar{g}_1+\frac{1}{(2\pi v)^3}[-11g_1^4+4g_1^2(g_1g_2-g_2^2)]\times\ln\left[\frac{\omega_D'}{\omega_D}\right], \tag{40}$$

$$g_2'=\bar{g}_2+\frac{1}{2(2\pi v)^3}[-11g_1^4+4g_1^2(g_1g_2-g_2^2)]\times\ln\left[\frac{\omega_D'}{\omega_D}\right]. \tag{41}$$

With the use of the invariant property $g_2'-\frac{1}{2}g_1'=g_2-\frac{1}{2}g_1$, the Lie equation for $g_1'$ becomes

$$\frac{\partial}{\partial x}\ln g_1'(x)=\frac{1}{x}\left[\frac{1}{\pi v}\left[1-\frac{\delta^2}{2}\right]g_1'(x)+\frac{g_1'^2(x)}{2(\pi v)^2}-\frac{5}{4(\pi v)^3}g_1'^3(x)\right]. \tag{42}$$

Here $\delta=(q_2-g_1/2)/\pi v$ and $x=vq/\omega_D$. In the weak-coupling limit where $\delta\ll 1$, $g_1<0$, and $q\to 0$, it is straightforward to show that $g_1'/\pi v$ scales to a fixed value $g_1'/\pi v=-\frac{1}{5}(\sqrt{21}-1)$ $(\simeq -0.716)$, which is quite different from the case where $\omega\to 0$ and $q=0$.

For $g_1<0$ we have reached the conclusion that the value of the invariant coupling $g_1'$ depends on the choice of the frequency and momentum variables for the vertex function. In the limit of weak coupling and $\omega\to 0$, $q=0$, $g_1'$ has the value $g_1'/\pi v\simeq -1.24$. In the other limit as $\omega=0$ and $q\to 0$, $g_1'$ scales to $g_1'/\pi v\simeq -0.716$. In order to evaluate the low-frequency response functions[5,7] which describe critical fluctuations of the singlet Cooper pairing, triplet Cooper pairing, spin-density wave, and charge-density wave, it seems that the value of $g_1'$ at $\omega\to 0$ and $q=0$ should be used. In this case, although the corrections from the vertex parts listed from graphs 1(a) to 1(e) to the invariant couplings are zero, the response functions using these graphs as vertex parts have finite value. Two of these response functions are shown in Figs. 2(a) and 2(b), in which external momentum and frequency variables appearing in the vertex part have to be integrated over and the result for each of them becomes finite. Moreover, it is doubtful whether the limit $\omega\to 0$ and $q=0$ should be used for the vertex parts listed from graphs 1(a) to 1(e), since the magnitude of the Landau bubble $L_B$ associated with each of these graphs, unlike those logarithmic divergent terms, depends critically on how $\omega$ and $q$ approach zero.[20] If we assume that only nonzero vertex parts contribute to the response functions, then there is a unique way to determine the values of graphs from 1(a) to 1(e). We have noticed that the value of graph 2(c) is identical to that of graph 2(b) except by a spin structure due to the interactions. Therefore, the vertex parts which enter graph 2(b) and 2(c) should have the same magnitude. Moreover, the vertex part which enters graph 2(c) is nonzero and together with its Cooper pairing counterpart, their contribution [graph 7(a) and 7(b) of Ref. 12] is given by[12] (see the Appendix)

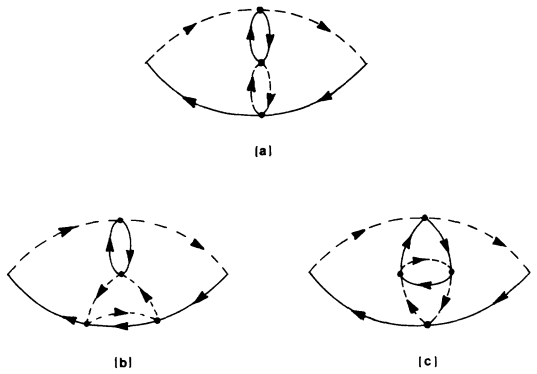


FIG. 2. Some graphs representing higher-order charge-density-wave or spin-density-wave response functions. Diagrams (a) and (b) use graphs 1(a) and 1(b) as vertex parts. Diagram (c) takes graph 7(a) of Ref. 12 as its vertex part.

$$\gamma^{(7ab)}(\omega)=(2g_1^4\delta_{\alpha\gamma}\delta_{\beta\delta}-g_1^4\delta_{\alpha\delta}\delta_{\beta\gamma})\times\frac{1}{(2\pi v)^3}\frac{1}{2}\ln\left[\frac{\omega}{\omega_D}\right]. \tag{43}$$

The correction to the vertex functions from graph 1(b)[21] and 1(c) can easily be shown to have the result

$$\gamma^{(1bc)}(\omega)=(2g_1^4\delta_{\alpha\gamma}\delta_{\beta\delta}-g_1^4\delta_{\alpha\delta}\delta_{\beta\gamma})\times\frac{L_B}{(2\pi v)^2}\frac{1}{2}\ln\left[\frac{\omega}{\omega_D}\right]. \tag{44}$$

$L_B$ here is given by Eq. (31) and it has different values in different limits. It is easy to show that the sum of the response functions with graphs 1(b) and 1(c) as vertex parts are equal to those with graphs 7(a) and 7(b) of Ref. 12 as vertex parts. Therefore, it is natural to choose[22] the value of $\gamma^{(1bc)}$ to be that of $\gamma^{(7ab)}$. This is equivalent to assigning $L_B=1/2\pi v$, or to take the limit $\omega=2vq\to 0$ for the Landau bubble in the present case. There should be no difficulty to show that the contribution from graphs 1(d) and 1(e) is identical with that of graphs 1(b) and 1(c), the final result[12] for them is written as

$$\gamma^{(1bcde)}(\omega)=(2g_1^4\delta_{\alpha\gamma}\delta_{\beta\delta}-g_1^4\delta_{\alpha\delta}\delta_{\beta\gamma})\times\frac{1}{(2\pi v)^3}\ln\left[\frac{\omega}{\omega_D}\right]. \quad (45)$$

It should be noted here that the above equation differs primarily from Eq. (33) by a minus sign. Graph 1(a) involves the product of two Landau bubbles, with $L_B=1/2\pi v$, its contribution can be easily obtained[12]:

$$\gamma^{(1a)}(\omega)=[g_1^3\delta_{\alpha\gamma}\delta_{\beta\delta}-(3g_1^2g_2-6g_1g_2^2+4g_2^3)\times\delta_{\alpha\delta}\delta_{\beta\gamma})]\frac{1}{(2\pi v)^2}. \quad (46)$$

By choosing the value of $L_B=1/2\pi v$, we wish to point out a simple fact that all the vertex parts, which are generated from an arbitrary vertex graph of lower order by replacing any of the black dots (bare interaction) with a zero-sound (or a Cooper-pairing) channel graph of two black dots, have the similar leading logarithmic divergent term except by a spin structure due to the interactions. With the use of Eqs. (45) and (46) as new contributions to the vertex functions, the constants $b_1$, $b_2$, $c_1$, and $c_2$ appearing in Eqs. (18) and (19) are, respectively, given by

$$\begin{aligned} b_1&=\frac{1}{(2\pi v)^3}[2g_1^3+4g_1(g_1g_2-g_2^2)],\\ b_2&=\frac{1}{(2\pi v)^3}\left[5g_1^3-\frac{g_1^2}{g_2}(\tfrac{1}{2}g_1^2+2g_2^2)\right],\\ c_1&=\frac{1}{(2\pi v)^2}g_1^2,\\ c_2&=\frac{1}{(2\pi v)^2}(3g_1^2-6g_1g_2+4g_2^2). \end{aligned} \quad (47)$$

From the multiplicative renormalization Eqs. (8) and (9), the constants $a_2$ and $a_3$ appearing in $z_2$ and $z_3$ can be obtained as

$$\begin{aligned} a_2&=\frac{1}{(2\pi v)^3}[-4g_1^3+4g_1(g_1g_2-g_2^2)],\\ a_3&=\frac{1}{(2\pi v)^3}\frac{1}{2g_2}[-7g_1^4+10g_1^3g_2-4g_1^2g_2^2]. \end{aligned} \quad (48)$$

From Eqs. (9) and (10), the invariant couplings $g_1'$ and $g_2'$ which should be used to calculate the low-frequency response function are given by

$$g_1'=\bar{g}_1+\frac{1}{(2\pi v)^3}[-7g_1^4+4(g_1^3g_2-g_1^2g_2^2)]\times\ln\left[\frac{\omega_D'}{\omega_D}\right], \quad (49)$$

$$g_2'=\bar{g}_2+\frac{1}{(2\pi v)^3}\tfrac{1}{2}[-7g_1^4+4(g_1^3g_2-g_1^2g_2^2)]\times\ln\left[\frac{\omega_D'}{\omega_D}\right]. \quad (50)$$

These expressions for $g_1'$ and $g_2'$ are identical with Eqs. (52) and (53) of Ref. 12 if the small term $\alpha$ is neglected there. It is noted that the above equations still satisfy the relation $g_2'-\frac{1}{2}g_1'=g_2-\frac{1}{2}g_1$. As we have shown in Ref. 12, for $g_1<0$ and weak couplings $g_1'$, which has been used for calculating the critical exponents of various response functions,[12] scales to fixed value $g_1'/\pi v\simeq-0.87$ in the low-frequency limit.

## IV. DISCUSSION

This paper is an extension of our previous work[12] for a one-dimensional Fermi system with weak-coupling parameters $g_1$ ($<0$) and $g_2$. All the relevant third- and fourth-order diagrams for the vertex parts and self-energies were evaluated in Ref. 12. In those calculations the momentum associated with each Green function appearing in every diagram had been restricted to the region $-k_c\le k\le k_c$. If there is no other profound reason the particle-hole symmetry should hold for this cutoff procedure.[23] By using the property of particle-hole symmetry, Fowler[13] was able to show that the value of $g_1-2g_2$ is scale invariant. In Ref. 12 the invariance of $g_1'-2g_1'$ was destroyed by the presence of the small term $\alpha$. The authors of the present paper have shown that this is due to insufficient accuracy in the calculation for the coefficient in front of the term $\ln(\omega/\omega_D)$ associated with some of the graphs in Fig. 5 of Ref. 12. This set of graphs has proven to be the most tedious to evaluate. Although the values for most of the graphs representing the vertex parts in Ref. 16 are identical with ours, there still remains minor differences for several graphs in addition to the major difference as pointed out in the text. We believe that these differences are due to the choice of different cutoff methods in momentum space.

The simplified results for the vertex parts listed in the Appendix of this paper can also be obtained by setting the external frequency equal to zero and inserting a cutoff $\omega/v$ (or $q$) near the origin in the region of momentum integration. With these results, we are able to show that the invariant coupling $g_1'$ scales to a fixed value $g_1'/\pi v\simeq-1.24$ in the limit $\omega\to0$, $q=0$ and it scales to $g_1'\pi v\simeq-0.716$ in the limit $\omega=0$, $q\to0$. For $g_1'>0$, there is no ambiguity and $g_1'/\pi v$ always scales to a very small value.[12] The reason that $g_1'$ scales to different values for $g_1'<0$ is because of the presence of the Landau bub-

bles [see graphs from 1(a) to 1(e)] in the third-order renormalization-group equation. As we have pointed out in Eq. (31), the magnitude of the Landau bubble, unlike the logarithmic divergent terms, critically depends on how $\omega$ and $q$ approach zero. On this basis we have argued that the invariant coupling which should be used to evaluate the critical exponents for various fluctuation response functions is from neither of the above limits but is given by $g_1'/\pi v \simeq -0.87$. The latter is obtained by assigning the value of the Landau bubble $L_B = 1/2\pi v$. The number $g_1'/\pi v \simeq -0.87$ should not be taken too seriously since its value is expected to change in a higher-order calculation. We are not sure whether the $\omega$- and $q$-dependent invariant couplings $g_1'$ and $g_2'$ should be interpreted as a breakdown of scaling in third order.

Finally, we would like to point out that the scaling equation for $g_1'$ [Eqs. (30) and (42)] depends on $g_2$ via the quantity $\delta$. This seems not to agree with the results obtained by using the Tomonaga's boson transformation, where the scaling equation for $g_1'$ does not contain $g_2$.[6,15] We believe that although both the model Hamiltonian used in this paper and the Hamiltonian obtained by bosonization of Eq. (2) describe the same system, the two are not exactly identical. Moreover, in the weak-coupling limit both models predict the same ground state.[12] Another consequence of our perturbative calculation is that the spin-density and the charge-density degrees of freedom may not be independent from each other.

## ACKNOWLEDGMENTS

One of us (C.-S. T.) would like to thank Dr. E. H. Rezayi for sending a copy of his paper (Ref. 16) prior to publication. This work is supported in part by ARO Contract No. DAAG 29-79-C10039.

## APPENDIX: LIST OF THE SIMPLIFIED RESULTS FOR THE VERTEX FUNCTIONS

The vertex $\Gamma$ can be decomposed into the following spin structure[4]:

$$\Gamma_{\alpha\beta,\gamma\delta}(\omega) = g_1 \tilde{\Gamma}_1(\omega)\delta_{\alpha\gamma}\delta_{\beta\delta} - g_2 \tilde{\Gamma}_2(\omega)\delta_{\alpha\delta}\delta_{\beta\gamma} . \tag{A1}$$

The first- and second-order corrections to $\tilde{\Gamma}_1$ and $\tilde{\Gamma}_2$ have been calculated previously.[4] If we neglect the imaginary parts and the constant terms due to the artificial effects,[19] $\tilde{\Gamma}_1$ and $\tilde{\Gamma}_2$ have the expressions

$$\tilde{\Gamma}_1^{(2)}(\omega) = 1 + \frac{g_1}{\pi v}\ln\left[\frac{\omega}{\omega_D}\right] + \frac{g_1^2}{(\pi v)^2}\ln^2\left[\frac{\omega}{\omega_D}\right] + \frac{1}{2(\pi v)^2}(g_1 g_2 - g_2^2)\ln\left[\frac{\omega}{\omega_D}\right] , \tag{A2}$$

$$\Gamma_2^{(2)}(\omega) = 1 + \frac{g_1^2}{\pi v}\frac{1}{2g_2}\ln\left[\frac{\omega}{\omega_D}\right] + \frac{g_1^3}{(\pi v)^2}\frac{1}{2g_2}\ln^2\left[\frac{\omega}{\omega_D}\right] + \frac{1}{(\pi v)^2}\frac{1}{4g_2}(g_1^3 - 2g_1^2 g_2 + 2g_1 g_2^2 - 2g_2^3)\ln\left[\frac{\omega}{\omega_D}\right] . \tag{A3}$$

In order to consider the third-order correction to $\tilde{\Gamma}_1$ and $\tilde{\Gamma}_2$ we need to know the fourth-order contribution to the vertex function $\Gamma(\omega)$. The fourth-order diagrams have been calculated previously.[12] Again if the imaginary parts and the terms due to artificial effects are neglected,[16,18] the fourth-order vertex parts in Fig. 5 of Ref. 12 can be rewritten in more simplified forms:

$$\gamma^{(5ab)}(\omega) = [4(2g_1^4 - 3g_1^3 g + 3g_1^2 g_2^2)\delta_{\alpha\gamma}\delta_{\beta\delta} - (6g_1^2 g_2^2 + g_1^4)\delta_{\alpha\delta}\delta_{\beta\gamma}]\frac{1}{(2\pi v)^3}\ln^3\left[\frac{\omega}{\omega_D}\right] , \tag{A4}$$

$$\gamma^{(5cd)}(\omega) = -[-8(g_1^3 g_2 - g_1^2 g_2^2)\delta_{\alpha\gamma}\delta_{\beta\delta} + 4(g_1^3 g_2 - g_1^2 g_2^2)\delta_{\alpha\delta}\delta_{\beta\gamma}]\frac{1}{2(2\pi v)^3}\ln^3\left[\frac{\omega}{\omega_D}\right] , \tag{A5}$$

$$\gamma^{(5ef)}(\omega) = -[-8(g_1^3 g_2 - g_1^2 g_2^2)\delta_{\alpha\gamma}\delta_{\beta\delta} + 4(g_1^3 g_2 - g_1^2 g_2^2)\delta_{\alpha\delta}\delta_{\beta\gamma}]\frac{1}{2(2\pi v)^3}\ln^3\left[\frac{\omega}{\omega_D}\right] , \tag{A6}$$

$$\gamma^{(5gh)}(\omega) = -[-2g_1^4\delta_{\alpha\gamma}\delta_{\beta\delta} + (4g_1^4 - 6g_1^3 g_2)\delta_{\alpha\delta}\delta_{\beta\gamma}]\frac{1}{3(2\pi v)^3}\ln^3\left[\frac{\omega}{\omega_D}\right] , \tag{A7}$$

$$\gamma^{(5ij)}(\omega) = -[-2g_1^4\delta_{\alpha\gamma}\delta_{\beta\delta} + (4g_1^4 - 6g_1^3 g_2)\delta_{\alpha\delta}\delta_{\beta\gamma}]\frac{1}{3(2\pi v)^3}\ln^3\left[\frac{\omega}{\omega_D}\right] , \tag{A8}$$

$$\gamma^{(5kl)}(\omega)=-[(4g_1^3g_2-4g_1^2g_2^2)\delta_{\alpha\gamma}\delta_{\beta\delta}+(3g_1^4-8g_1^3g_2+2g_1^2g_2^2)\delta_{\alpha\delta}\delta_{\beta\gamma}]\frac{1}{3(2\pi v)^3}\ln^3\left[\frac{\omega}{\omega_D}\right], \tag{A9}$$

$$\gamma^{(5mn)}(\omega)=-[-8(g_1^3g_2-g_1^2g_2^2)\delta_{\alpha\gamma}\delta_{\beta\delta}+4(g_1^3g_2-g_1^2g_2^2)\delta_{\alpha\delta}\delta_{\beta\gamma}]\frac{1}{3(2\pi v)^3}\ln^3\left[\frac{\omega}{\omega_D}\right], \tag{A10}$$

$$\gamma^{(5op)}(\omega)=-[2(g_1^4-2g_1^3g_2+2g_1^2g_2^2)\delta_{\alpha\gamma}\delta_{\beta\delta}-(g_1^4-2g_1^3g_2+2g_1^2g_2^2)\delta_{\alpha\delta}\delta_{\beta\gamma}]\frac{1}{6(2\pi v)^3}\ln^3\left[\frac{\omega}{\omega_D}\right], \tag{A11}$$

$$\gamma^{(5qr)}(\omega)=-[2(g_1^4-2g_1^3g_2+2g_1^2g_2^2)\delta_{\alpha\gamma}\delta_{\beta\delta}-(g_1^4-2g_1^3g_2+2g_1^2g_2^2)\delta_{\alpha\delta}\delta_{\beta\gamma}]\frac{1}{6(2\pi v)^3}\ln^3\left[\frac{\omega}{\omega_D}\right], \tag{A12}$$

$$\gamma^{(5st)}(\omega)=-[2(g_1^4-2g_1^3g_2+2g_1^2g_2^2)\delta_{\alpha\gamma}\delta_{\beta\delta}-(g_1^4-2g_1^3g_2+2g_1^2g_2^2)\delta_{\alpha\delta}\delta_{\beta\gamma}]\frac{1}{6(2\pi v)^3}\ln^3\left[\frac{\omega}{\omega_D}\right], \tag{A13}$$

$$\gamma^{(5uv)}(\omega)=-[2(g_1^4-2g_1^3g_2+g_1^2g_2^2)\delta_{\alpha\gamma}\delta_{\beta\delta}-(g_1^4-2g_1^3g_2+2g_1^2g_2^2)\delta_{\alpha\delta}\delta_{\beta\gamma}]\frac{1}{6(2\pi v)^3}\ln^3\left[\frac{\omega}{\omega_D}\right]. \tag{A14}$$

The next class of graphs comes from Fig. 6 of Ref. 12; they can be rewritten as

$$\gamma^{(6abcd)}(\omega)=2(g_1^2-g_1g_2+g_2^2)(2g_1^2\delta_{\alpha\gamma}\delta_{\beta\delta}-g_1^2\delta_{\alpha\delta}\delta_{\beta\gamma})\frac{1}{2(2\pi v)^3}\left[\ln^2\left[\frac{\omega}{\omega_D}\right]-\ln\left[\frac{\omega}{\omega_D}\right]\right], \tag{A15}$$

$$\gamma^{(6ef)}(\omega)=[-4g_1^2(g_2^2-g_1g_2)\delta_{\alpha\gamma}\delta_{\beta\delta}+2g_1^2(g_2^2-g_1g_2)\delta_{\alpha\delta}\delta_{\beta\gamma}]\frac{1}{4(2\pi v)^3}\left[\ln^2\left[\frac{\omega}{\omega_D}\right]-\ln\left[\frac{\omega}{\omega_D}\right]\right], \tag{A16}$$

$$\gamma^{(6gh)}(\omega)=[-4g_1^2(g_2^2-g_1g_2)\delta_{\alpha\gamma}\delta_{\beta\delta}+2g_1^2(g_2^2-g_1g_2)\delta_{\alpha\delta}\delta_{\beta\gamma}]\frac{1}{4(2\pi v)^3}\left[\ln^2\left[\frac{\omega}{\omega_D}\right]-\ln\left[\frac{\omega}{\omega_D}\right]\right], \tag{A17}$$

$$\gamma^{(6ijkl)}(\omega)=[(4g_1^3g_2-4g_1^2g_2^2)\delta_{\alpha\gamma}\delta_{\beta\delta}-(2g_1^3g_2-2g_1^2g_2^2)\delta_{\alpha\delta}\delta_{\beta\gamma}]\frac{1}{2(2\pi v)^3}\left[\ln^2\left[\frac{\omega}{\omega_D}\right]+\ln\left[\frac{\omega}{\omega_D}\right]\right], \tag{A18}$$

$$\gamma^{(6mnop)}(\omega)=[(4g_1^3g_2-4g_1^2g_2^2)\delta_{\alpha\gamma}\delta_{\beta\delta}-(2g_1^3g_2-2g_1^2g_2^2)\delta_{\alpha\delta}\delta_{\beta\gamma}]\frac{1}{2(2\pi v)^3}\left[\ln^2\left[\frac{\omega}{\omega_D}\right]+\ln\left[\frac{\omega}{\omega_D}\right]\right], \tag{A19}$$

$$\gamma^{(6qrst)}(\omega)=[g_1^4\delta_{\alpha\gamma}\delta_{\beta\delta}-(2g_1^4-3g_1^3g_2)\delta_{\alpha\delta}\delta_{\beta\gamma}]\frac{1}{2(2\pi v)^3}\left[\ln^2\left[\frac{\omega}{\omega_D}\right]-\ln\left[\frac{\omega}{\omega_D}\right]\right], \tag{A20}$$

$$\gamma^{(6uvwx)}(\omega)=[g_1^4\delta_{\alpha\gamma}\delta_{\beta\delta}-(2g_1^4-3g_1^3g_2)\delta_{\alpha\delta}\delta_{\beta\gamma}]\frac{1}{2(2\pi v)^3}\left[\ln^2\left[\frac{\omega}{\omega_D}\right]-\ln\left[\frac{\omega}{\omega_D}\right]\right] \tag{A21}$$

The last set of graphs are shown in Fig. 7 of Ref. 12; they have the following expression[12]:

$$\gamma^{(7ab)}(\omega)=(2g_1^4\delta_{\alpha\gamma}\delta_{\beta\delta}-g_1^4\delta_{\alpha\delta}\delta_{\beta\gamma})\frac{1}{2(2\pi v)^3}\ln\left[\frac{\omega}{\omega_D}\right], \tag{A22}$$

$$\gamma^{(7cdef)}(\omega)=(2g_1^4\delta_{\alpha\gamma}\delta_{\beta\delta}-g_1^4\delta_{\alpha\delta}\delta_{\beta\gamma}\frac{1}{(2\pi v)^3}\ln\left[\frac{\omega}{\omega_D}\right], \tag{A23}$$

$$\gamma^{(7kl)}=0. \tag{A24}$$

The contribution from graphs 7(g)–7(j) is zero in the limit $\omega\to 0$, $q=0$. By summing the right-hand sides of Eqs. (A4)–(A24) together with Eqs. (A2) and (A3), it is straightforward to show that the vertex functions $\tilde{\Gamma}_1(\omega)$ and $\tilde{\Gamma}_2(\omega)$ are, respectively, given by Eqs. (18) and (19) with constants $b_1$ and $b_2$ defined in Eqs. (24) and (25), and constants $c_1=c_2=0$.

[1]J. A. Bychikov, L. P. Gorkov, and I. E. Dzyaloshinsky, Zh. Eksp. Teor. Fiz. 50, 738 (1966) [Sov. Phys.—JETP 23, 489 (1966)].
[2]E. H. Lieb and F. Y. Wu, Phys. Rev. Lett. 20, 1445 (1968).
[3]I. E. Dzaloshinsky and A. I. Larkin, Zh. Eksp. Teor. Fiz. 61, 791 (1971) [Sov. Phys.—JETP 34, 422 (1972)].
[4]N. Menyhárd and J. Sólyom, J. Low Temp. Phys. 12, 529 (1973).
[5]J. Sólyom, J. Low Temp. Phys. 12, 547 (1973).
[6]A. Luther and V. J. Emery, Phys. Rev. Lett. 33, 589 (1974).
[7]H. Fukuyama, T. M. Rice, C. M. Varma, and B. I. Halperin, Phys. Rev. B 10, 3775 (1974).
[8]M. Konishi and M. Kimura, Prog. Theor. Phys. 52, 353 (1974).
[9]A. Luther and I. Peschel, Phys. Rev. B 9, 2911 (1974).
[10]P. A. Lee, Phys. Rev. Lett. 34, 1247 (1975).
[11]J. Sólyom, Solid State Commun. 17, 63 (1975).
[12]C. S. Ting, Phys. Rev. B 13, 4029 (1976).
[13]M. Fowler, Solid State Commun. 18, 241 (1976).
[14]V. N. Prigodin and Yu. A. Firsov, Zh. Eksp. Teor. Fiz. 71, 2252 (1976).
[15]A. I. Larkin and J. Sak, Phys. Rev. Lett. 39, 1025 (1977).
[16]E. H. Rezayi, J. Sak, and S. Talukdar, Phys. Rev. B 19, 4757 (1979).
[17]N. N. Bogoliubov and D. V. Shirkov, *Introduction to Theory of Quantized Fields* (Interscience, New York, 1959).

[18]Since $g_1' - \frac{1}{2}g_2'$ is scale invariant (see Ref. 13), the terms due to the artificial effects should be canceled.

[19]If we temporarily neglect the contribution from graph 4(i), the constant terms $C_1(g)$ and $C_2(g)$ in Eqs. (24) and (25) of Ref. 12 are entirely due to artificial effects. Moreover, $\tilde{\Gamma}_2^{(2)}$ defined in Eq. (25) of Ref. 12 has a typographical error, namely the coefficient in front of $[\ln^2(\omega/\omega_D) - i\pi\ln(\omega/\omega_D)]$ should be $2g_1^3/(2\pi v)^2 g_2$, not $2g_1^2/(2\pi v)^2$.

[20]In Ref. 12 we obtained the result for the Landau bubble by integrating over the momentum variable first. For example,

$$L_B = \frac{1}{2\pi v}\frac{1}{2\pi i}\int_{-\infty}^{\infty} d\omega' \int_{-vk_c}^{vk_c} \frac{d\xi}{[\omega'+\omega-\xi+i\delta\,\mathrm{sgn}(\omega'+\omega)][\omega'-\xi+i\delta\,\mathrm{sgn}(\omega')]} .$$

It is straightforward to show that with fixed $vk_c$, $L_B=0$. But if $vk_c$ is extended to $\infty$, the method of contour integration can be used. $L_B$ is nonzero only when $\omega'+\omega>0$ and $\omega'<0$. We then obtain $L_B=1/2\pi v$. By doing this we have neglected the contribution from large $\xi$. This type of integration has been used extensively for studying the electronic transport in metals. [See A. A. Abrikosov, L. P. Górkov, and I. Ye. Dzyaloshinskii, *Quantum Field Theoretical Methods in Statistical Physics* (Pergamon, Oxford, 1965), pp. 328 and 329.

[21]Graph 1(b) is the vertex part which enters the response function as shown in graph 2(b).

[22]Graphs 1(b)–1(e) of the present paper and graphs 7(a) and 7(b) of Ref. 12 can be obtained from graph 1(a) of the present paper simply by replacing one of its black dots (bare interaction) with a Cooper pairing (or zero-sound channel) diagram.

[23]K. G. Wilson (private communication).